(Online) ISSN 2744-1741
Defense and Security Studies *Original Research*
Vol. 7, No. 1, 2026, pp.1-21
https://doi.org/10.37868/dss.v7.id302

Design and analysis of a wideband split-ring integrated hybrid fractal-shaped patch antenna for WiFi, WiMAX, WLAN/5G midband applications

K. Rani Rudrama[1*], Md. Shoaib[2], P. Anjali[3], T. Divya Sri Sivatmika[4]
[1,2,3,4] Electronics and Communication Engineering, Lakireddy Bali Reddy College of Engineering, India

*Corresponding author E-mail: kodali.rudrama@gmail.com

Received: Dec. 3, 2025
Revised: Jan. 10, 2026
Accepted: Jan. 11, 2026
Online: Jan.12, 2026

Abstract

A split-ring integrated hybrid fractal antenna has been designed with improved bandwidth from 3 GHz to 9.56 GHz and is presented for WiFi/WiMAX/WLAN/5G midband applications. The proposed antenna is planned to deliver an extended bandwidth and is consists of split-ring resonators integrated with a fractal-shaped patch. The Fractal Shape in the antenna provides a compact size due to its self-similarity, space-filling property, and additional split-ring resonators to improve the bandwidth. The antenna, compact in size with dimensions of 31×37mm^2 and a thickness of 1.8mm, is constructed upon an FR4 epoxy substrate showing a dielectric constant of 4.4. The proposed antenna performance is presented with the help of reflection coefficient and VSWR plots, gain, field distribution, and radiation pattern. The comparison of simulated and measured analysis and results showed good agreement, indicating that the design antenna is suitable for WiFi, WiMAX, WLAN, and 5G applications.

Keywords: wideband antenna, split-ring resonators, fractal geometry

1. Introduction

Antennas are crucial components of contemporary wireless communication systems because they guarantee low return loss, omnidirectional radiation patterns, high performance over large bandwidths, and increased gain. As new technologies demand more affordable, smaller solutions, antenna designs need to be efficient while reducing cross-polarization. In this regard, Mandelbrot's introduction of fractal geometries in 1975 [1] revolutionized antenna design. They are perfect for applications like WiFi, WiMAX, WLAN, and 5G networks because of their skill to maintain similar patterns and effectively occupy space allows for better compactness and bandwidth [2, 3].

A variety of fractal geometries have been studied in an effort to improve antenna performance. Koch-like fractal curves have been used in PCS, WLAN, WiFi, and WiMAX applications [5], For example, an octagonal fractal microstrip patches antenna, for example, has a super wideband range of 10 GHz to 50 GHz [4]. An ultrawideband (UWB) antenna was created by mixing a Pythagorean tree into a T-patch [6]. Additional developments contain the use of fractal structures to enhance the performance of dielectric resonator antennas [8–13] and Sierpinski carpet antennas in combination with grounded coplanar waveguides, which have been demonstrated to increase bandwidth [7].

Construction on these developments, hybrid fractal designs have demonstrated remarkable improvements, especially in wideband or multiband performance and antenna reduction. For instance, patch antennas that use Koch curves and Sierpinski carpets have achieved a balance between reduced size and improved bandwidth [6]. Additional alterations, like slotted ground planes in conjunction with disturbed Sierpinski fractals, have also proven successful in GSM, WLAN, and USB dongle applications [7]. These hybrid geometries, such as Koch-Minkowski combinations, offer improved efficiency along with compact designs, which makes them appropriate for contemporary applications like WiMAX and ISM bands [3-6]. These developments demonstrate how fractal-inspired designs can be used to overcome the difficulties presented by next-generation communication systems.

Advanced fractal antenna designs for 5G and other technologies have been the subject of recent research. For 5G mmWave applications, Azari et al. Presented a super wideband dual polarized Vivaldi antenna that showed dual-polarization capabilities and a broad frequency range [17]. To enhance antenna performance, Li et al. suggested a broadband circularly polarized microstrip antenna with a folded split-ring resonator [18].

By stacking magneto-dielectric composites and split-ring resonators, Adhiyoga et al. produced a small 5G antenna with higher gain [19]. Yang et al. demonstrated a multimode resonance-based wideband diversity cylindrical dielectric resonator antenna [21], while Pradhan et al. suggested a high-isolation HMSIW-based self-triplexing antenna for WiFi and WLAN [20]. For 5G mobile terminals, Wang and Wu also created wideband MIMO antennas, which boost channel capacity while reducing interference [22].

A split-ring integrated hybrid fractal antenna with improved bandwidth for WLAN, 5G midband, WiMAX, and WiFi applications is proposed in this study. With dimensions of 31 × 37 mm² and a thickness of 1.8 mm, the antenna is small and covers the operating frequency range of 3 GHz to 9.56 GHz. A fractal-shaped patch and split-ring resonators work together to boost bandwidth while keeping the form factor small. A FR4 epoxy substrate with a dielectric constant of 4.4 serves as the foundation for the antenna.

Plots of the reflection coefficient, VSWR, gain, field distribution, and radiation patterns are used to prove its performance. Exceptional agreement between simulation and measurement validates that the antenna is appropriate for WLAN, 5G, WiMAX, and WiFi applications. This hybrid fractal design addresses the growing need for compact, high-performance antennas in modern communication systems and holds promise for advancements in IoT, satellite systems, and 5G technologies.

1.1 Literature review

The development of compact, multi-band antennas has gathered a lot of attention in recent years, particularly for applications such as WLAN, WiMAX, WiFi, and the upcoming 5G mid-band communications. Fractal geometries and split-ring resonators (SRRs) have become effective tools for enhancing antenna performance, offering miniaturization, multiband operation, and higher gain. The contributions from earlier research that serve as the basis for our paper are emphasized in this review of the literature, which looks at pertinent work in this field. WLAN and WiMAX applications using hybrid and wideband fractal antennas. M. Rauf and A.Jamil [1] made a proposal.

WLAN applications use a wideband hybrid fractal ring antenna, with a focus on hybrid fractal designs for efficiency, compactness, and wideband characteristics. In a similar vein, Dhirgham K. Naji [5] showed how fractal geometries can improve performance by creating a dual-band fractal ring antenna that is optimized for WLAN and WiMAX. A super wideband dual-polarized Vivaldi antenna was used by Azari et al. [17] to validate 5G mm Wave applications, showcasing both its dual-polarization capabilities and wide frequency range. In order to solve problems with channel capacity and interference mitigation, Wang and Wu [22] developed wideband MIMO antennas for 5G mobile terminals.

Antennas Based on Split-Ring Resonators (SRR) Wideband and multiband designs heavily depend on on SRRs. In order to create hybrid antennas that support multiple bands, Narinder Sharma and Sumeet Singh Bhatia [2]

combined SRRs with fractal geometries. A Minkowski fractal multiband antenna with circular SRRs was presented by Rajkumar Rengasamy and Dileepan Dhanasekaran [3], demonstrating novel geometries for improved performance. For WLAN/WiMAX applications, while Zheng et al. [8] proposed a tri-band ultra-wideband antenna with deformed SRRs, illustrating the versatility of SRRs. By creating a tilted beam broadband circularly polarized microstrip antenna and using folded SRRs to enhance overall performance, Li et al. [18] made an additional contribution.

Small Broadband Antennas A compact wideband printed IFA with electromagnetic band-gap structures was created by Dalia M. Elsheakh and Esmat A. Abdallah [9], demonstrating size reduction without sacrificing functionality. To meet the demand for wide frequency coverage, Mohamed Marzouk and Youssef Rhazi [6] presented a small fractal ultra-wideband antenna for WLAN, WiMAX, and other bands. In order to achieve improved gain and compactness, Adhiyoga et al. [19] used a stacked SRR structure with magneto-dielectric composite material to design a miniaturized 5G antenna.

Fractals and DGS in Advanced Antenna Designs Antennas such as the dual-frequency Sierpinski fractal geometry [11] and the multiband E-shaped fractal microstrip patch antenna [10] have shown notable improvements in bandwidth and gain by incorporating advanced fractal geometries and defected ground structures (DGS). Miniaturized wideband designs have also been investigated by combining fractal geometries like Sierpinski and Minkowski [12]. In order to improve diversity performance, Yang et al. [21] designed a wideband diversity cylindrical dielectric resonator antenna that utilizes multimode resonance.

Contribution to our work in this study expands on these research by introducing a wideband hybrid fractal patch antenna integrated with split-ring structures that is personalized for WLAN, 5G mid-band, WiMAX, and WiFi applications. SRR is inserted into hybrid fractal geometries to produce a small design with improved wideband performance and gain.

2. Antenna design

2.1 Antenna model

The planned split-ring integrated hybrid fractal antenna is illustrated in Figure 1. To increase bandwidth, a defected ground structure (DGS) is added to the bottom ground plane. The antenna uses split-ring resonators (SRRs) in a fractal patch to improve performance. A 50 Ω microstrip transmission line supplies power to the antenna. The substrate is composed of FR4 epoxy, which make available mechanical stability and efficient signal transmission, and have a thickness of 1.8 mm and a relative permittivity of 4.4.

Through excitation of the radiating element, the DGS optimizes radiation characteristics and impedance matching. Standard microstrip patch antenna equations were used to determine the patch's dimensions. The antenna is appropriate for contemporary wireless communication systems due to its high gain and effective radiation, which are achieved within the frequency range of 3 GHz to 9.56 GHz.

Tables 1 and 2 provide specifics about the proposed antenna's dimensions and design parameters, respectively. In order to ensure accurate replication and analysis of the antenna's performance, these tables offer thorough measurements of the patch, ground plane, SRRs, and feedline. The corresponding image of the antenna is shown in Figure 1.

Table 1 Design Parameters

Parameters	Representation	Value
Dielectric constant	ε_r	4.2
Loss tangent	tan σ	0.02
Thickness	h	1.8 mm

Table 2 Design values of patch antenna

Parameters	Symbol	Value
Operating frequency	f_o	2.45 GHz
Substrate thickness	h	1.8 mm
Size of ground	D_g	31 mm
Side of Triangle	T_s	2.5 mm
Size of substrate	W_s	31 mm
Size of substrate	Ls	37 mm
Feed Width	W_f	2 mm
Feed length	L_f	14.5 mm
Patch width	W_p	22 mm
and length	L_p	18 mm
Substrate dielectric constant	ϵ_r	4.2
Input impedance	Z_o	50Ω

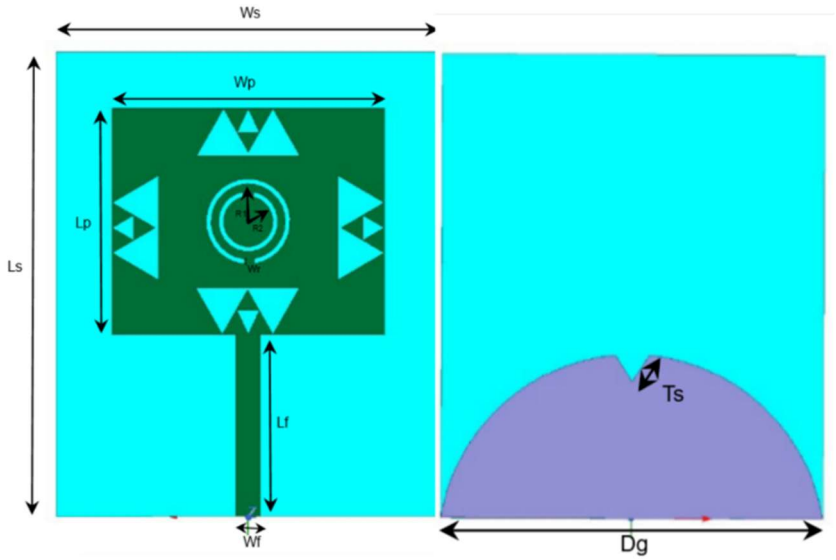

Figure 1. Proposed WB antenna a) Front view b) Rear view

The following formula yields the fundamental resonant frequency:

$$f_r = \frac{144}{L_1+L_2+\frac{A1}{2\pi L_1\sqrt{\varepsilon_{re}}}+\frac{A2}{2\pi L_2\sqrt{\varepsilon_{re}}}} \quad (1)$$

where,
L_1= Length of the ground plane
L_2=Length of the radiating patch
A_1=Area of the ground plane
A_2=Area of the radiation patch
ε_{re} = Effective dielectric constant.

The dimensions used to create the proposed WB antenna are listed in the Table 2.

2.2 Antenna evolution

2.2.1 First iteration

In the initial stage of the antenna development, the developed antenna design was conceptualized with the goal of achieving wideband performance appropriate for a range of communication uses.

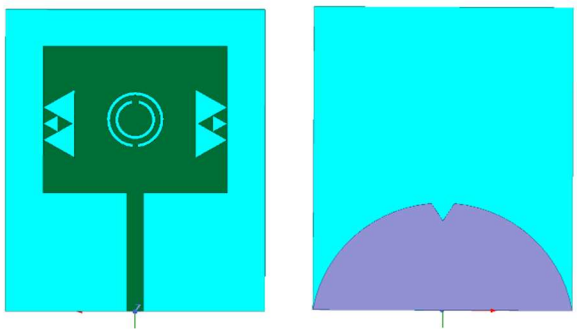

Figure 2. 1st Iteration a) Front view b) Rear view

The antenna, as shown in Figure 2, was designed, and analysed to evaluate its initial performance. The S-parameter graph in Figure 3 shows the performance of the antenna, showing that was operational within a specified frequency band.

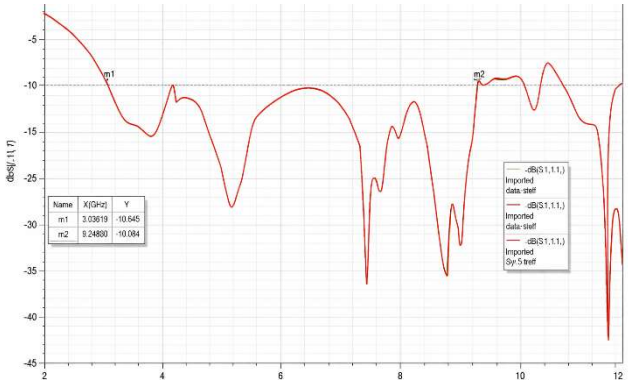

Figure 3. S-parameters graph of 1st iteration

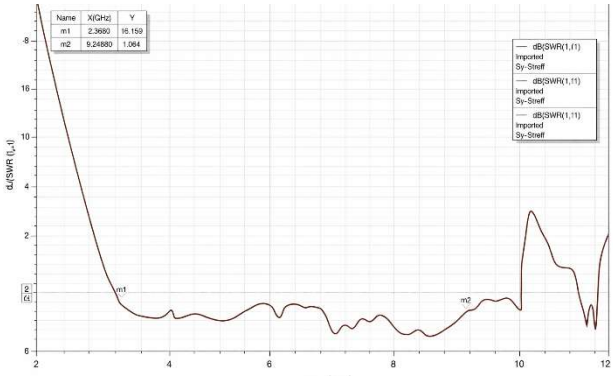

Figure 4. VSWR graph of 1st iteration

Following the initial analysis, The antenna's frequency range was determined to be 3.049 GHz to 9.288 GHz, offering a wide conduction band suitable for communication systems. However, the VSWR graph in Figure 4 indicates that impedance matching is not optimal across the entire frequency range. In some parts of the band, VSWR values exceed the ideal 1:1 ratio, suggesting potential power transmission losses that could be improved through further optimization.

2.2.2 Second iteration

In the second iteration of antenna development, several modifications were introduced to enhance performance. These adjustments focused on improving impedance matching and reducing VSWR across the entire frequency band. The updated design was analyzed to assess the impact of these changes, as illustrated in Figure 5.

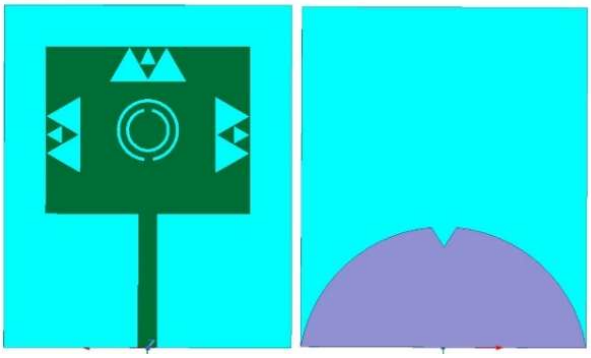

Figure 5. 2nd Iteration a) Front view b) Rear view

The S-parameter graph in Figure 6 shows the antenna's performance after modifications, showing an improved conduction band.

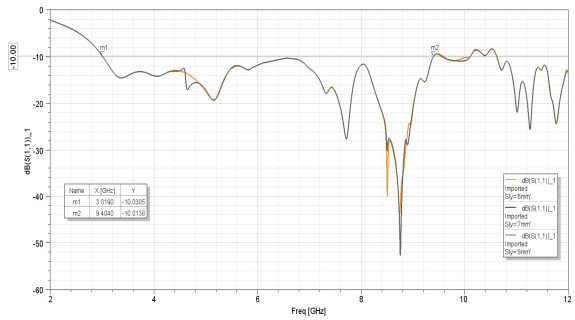

Figure 6. S-parameters graph of 2nd iteration

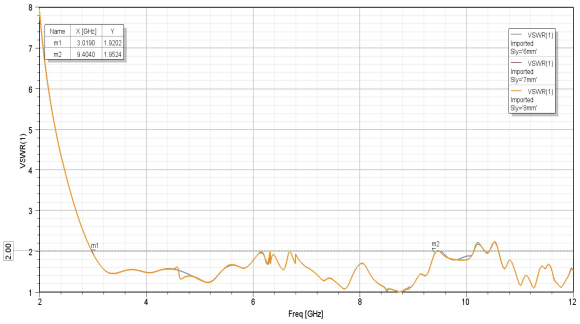

Figure 7. VSWR graph of 2nd iteration

Following this, the frequency range of the antenna was refined and now spans from 3.019 GHz to 9.404 GHz, offering a broader and more optimized bandwidth compared to the initial design. The VSWR graph in Figure 7 further demonstrates the improvements, with significantly reduced values across most of the frequency range. The impedance matching has been improved, leading to a more effective power transfer, and improved overall performance of the antenna.

2.2.3 Third iteration

The developed antenna's final design was established after thorough iterations to maximize efficiency and guarantee the best impedance matching across the whole range of frequencies. The antenna, as displayed in Figure 8, was tested to evaluate the performance improvements made through the previous modifications.

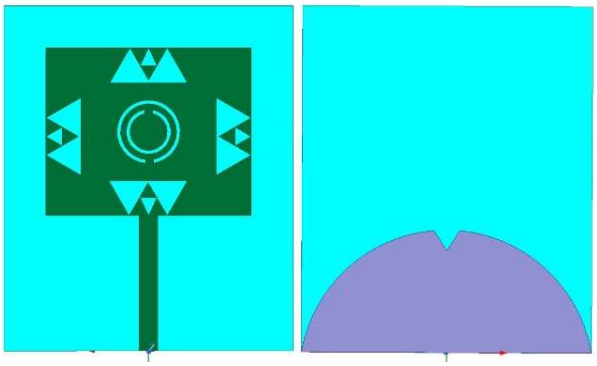

Figure 8. 3rd Iteration a) Front view b) Rear view

The S-parameter graph in Figure 9 reveals the enhanced antenna performance, with a well-defined conduction band. The range of frequencies of the proposed antenna was finalized to length from 3.025 GHz to 9.566 GHz, offering an even broader bandwidth compared to the previous iterations.

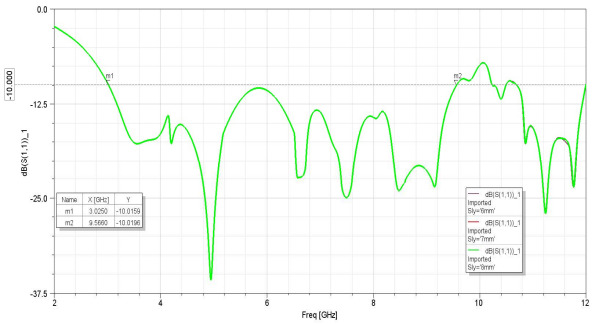

Figure 9. S-parameters graph of 3rd iteration

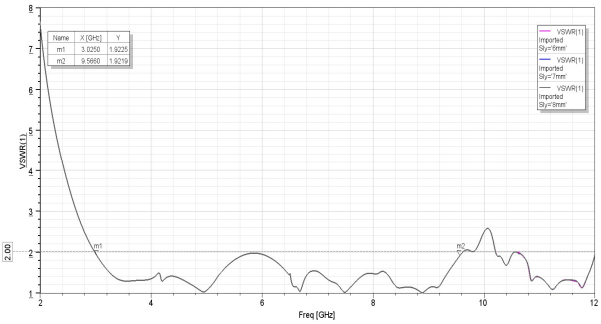

Figure 10. VSWR graph of 3rd iteration

Additionally, the VSWR graph in Figure 10 proves significant improvement in impedance matching throughout the entire frequency spectrum. The optimized antenna now shows a lower and more consistent VSWR, ensuring better efficiency in power transfer and further enhancing the antenna's overall performance.

Throughout the development process of the proposed antenna, each iteration resulted in a noticeable increase in the bandwidth, demonstrating the effectiveness of the modifications.

- In the first iteration, the bandwidth was 6.239 GHz (ranging from 3.049 GHz to 9.288 GHz).
- In the second iteration, the bandwidth increased to 6.385 GHz(ranging from 3.019 GHz to 9.404 GHz), showing an improvement of 0.146 GHz.
- Finally, for the proposed antenna, the bandwidth reached 6.541 GHz (from 3.025 GHz to 9.566 GHz), with an additional increase of 0.156 GHz.

This development of bandwidth increases highlights the continuous fine-tuning and improvement of the antenna design, ensuring better performance and broader frequency coverage at each step.

2.3 Gain and radiation pattern of developed antenna

The proposed antenna's gain provides key insights into its radiation performance over 3.025 GHz to 9.566 GHz. It achieves a maximum gain of 19.02 dB, an average of 5.12 dB, and a minimum of -23.75 dB. The negative gain occurs due to proximity to lossy materials like human tissue or clothing, which absorb energy and reduce efficiency (Figures 11 and 12).

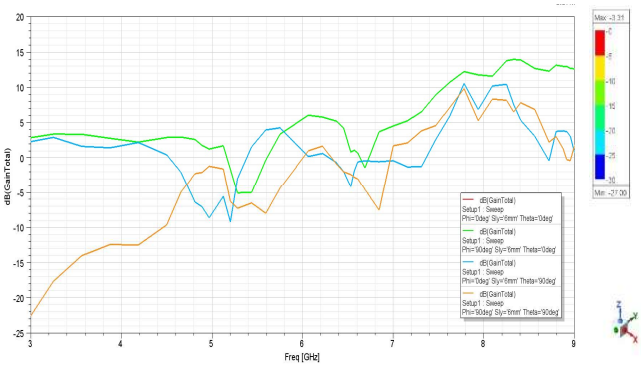

Figure 11. Simulated 2D Gain

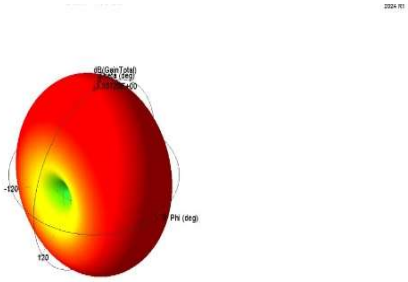

Figure 12. Simulated 3D Gain

The antenna accomplishes positive gain in most scenarios, ensuring reliable performance for WiFi, WiMAX, WLAN, and 5G midband applications. Its far-field radiation pattern (Fig. 13) shows an omnidirectional response with maximum radiation at 0°, ensuring uniform coverage. With compact dimensions of 31 × 37 mm, it is well-suited for wearable and portable devices. The design effectively balances compactness, wideband operation, and gain to meet modern wireless communication needs. Additionally, the antenna's radiation pattern was analysed to assess performance across different frequencies and angles.

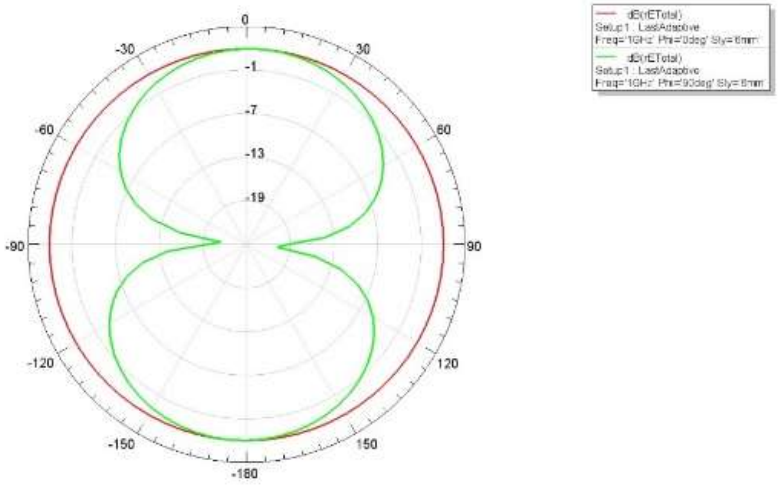

Figure 13. Simulated antenna's radiation pattern

The study measured the total radiated electric field (rETotal) in dB over a range of theta angles (0°–360°) and phi angles at different frequencies. Results show that the antenna maintains stable and consistent radiation features across these angles, ensuring reliable far-field performance. The radiation pattern exhibits both omnidirectional and directional behaviour, providing uniform coverage and efficient energy distribution. Additionally, the antenna withstands steady radiation intensity over its wide frequency band, making it well-suited for modern wireless applications such as WiFi, WiMAX, WLAN, and 5G midband. Its combination of wideband operation and strong radiation performance ensures high efficiency and reliable connectivity..

3. Fabrication results

The manufactured antenna was tested, with results shown in Figures 15 and 16 for return loss and VSWR. The return loss (Figure 15) confirms wideband functionality from 3.025 to 9.566 GHz, maintaining values below -10 dB, indicating excellent impedance alignment and high radiation efficiency.

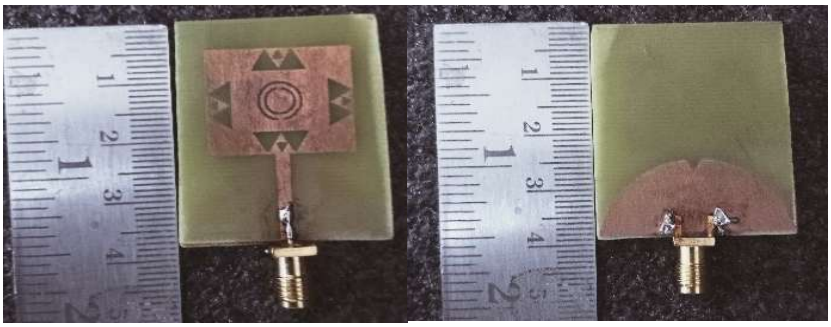

Figure 14. a) Front view b) Rear view

The VSWR plot (Figure 16) confirms the antenna's effectiveness, with values consistently below 2 across the operating band. However, compared to simulations, the measured results shifted slightly lower due to manufacturing tolerances and variations in the experimental setup.

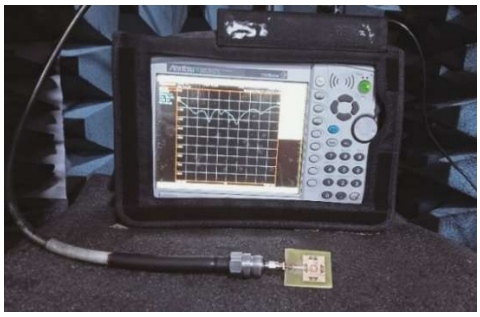

Figure 15. Return loss

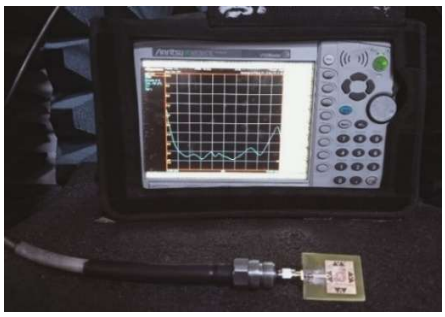

Figure 16. VSWR

Despite minor differences, the fabricated antenna's performance aligns with simulated results, confirming its suitability for WiFi, WiMAX, WLAN, and 5G midband applications.

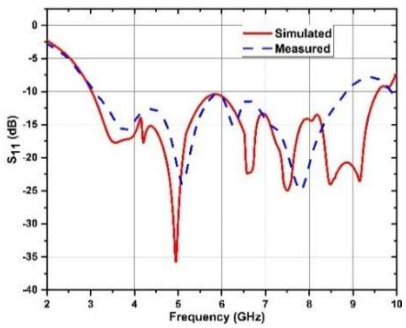

Figure 17. Return loss

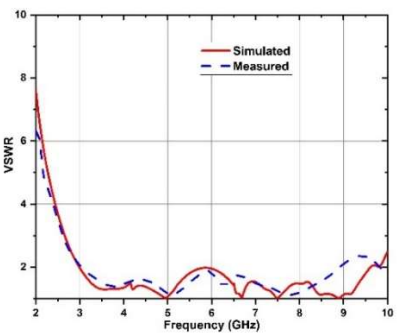

Figure 18. VSWR

The measured gain (Figure 19) closely matches simulations, ensuring stable and efficient radiation performance.

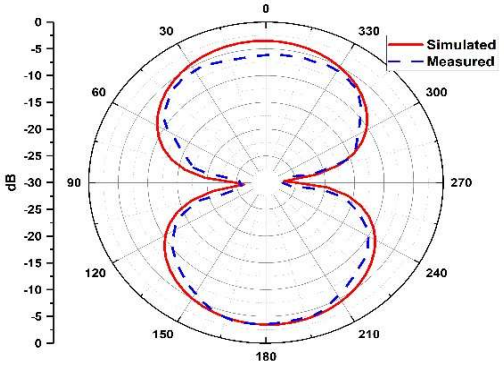

Figure 19. Measurement of gain

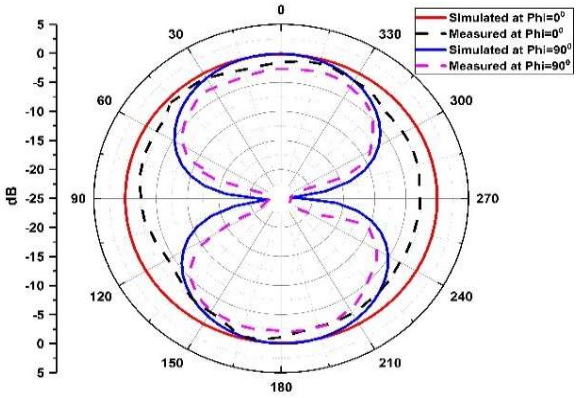

Figure 20. Measurement of radiation pattern

The measured radiation pattern (Figure 20) closely matches the simulation, ensuring effective performance for the intended applications. Minor variations in gain and radiation pattern are due to fabrication tolerances and testing conditions, but the antenna meets performance requirements, validating its design.

4. Conclusion

The design, analysis, and optimization of a wideband split-ring integrated hybrid fractal-shaped patch antenna for WLAN, 5G midband, WiMAX, and WiFi applications are the main objectives of this study. High data rates and compatibility with multiple standards are guaranteed by the small 31 × 37 mm antenna, which operates between 3.025 GHz and 9.566 GHz, reaching a bandwidth of 6.541 GHz. The FR4 epoxy substrate was selected because it improves efficiency and radiation characteristics while striking a balance between performance and manufacturing feasibility. Impedance matching and radiation patterns were enhanced by the split-ring integration and hybrid fractal shape. The antenna's remarkable wideband capability, efficiency, and gain made it appropriate for use in contemporary communication systems.

Future work may explore miniaturization techniques to reduce size while maintaining performance. Efficiency may be improved by using high-frequency or low-loss substrates, particularly at higher frequencies. Further optimization of radiation and bandwidth may be possible with advanced metamaterials or fractal geometries. Reliability for commercial deployment will be evaluated through environmental testing in varying temperatures and humidity levels. For new wireless technologies, assessing multi-band compatibility is essential to guaranteeing wider applications in next-generation communication systems.

References

[1] A. Jamil and M. Rauf, "A wideband hybrid fractal ring antenna for WLAN applications," *International Journal of Antennas and Propagation*, vol. 2022, Art. no. 6136916, 2022. https://doi.org/10.1155/2022/6136916

[2] N. Sharma and S. S. Bhatia, "Split ring resonator based multiband hybrid fractal antennas for wireless applications," *Progress in Electromagnetics Research*, 2018. https://doi.org/10.2528/PIERM18052403

[3] R. Rengasamy and D. Dhanasekaran, "Modified Minkowski fractal multiband antenna with circular-shaped split-ring resonator for wireless applications," *Measurement*, vol. 178, Art. no. 109766, 2021. https://doi.org/10.1016/j.measurement.2021.109766

[4] C. Elavarasi and T. Shanmuganantham, "Multiband SRR loaded Koch star fractal antenna," *Alexandria Engineering Journal*, vol. 57, no. 2, pp. 845–852, 2018. https://doi.org/10.1016/j.aej.2017.04.001

[5] D. K. Naji, "Compact design of dual-band fractal ring antenna for WiMAX and WLAN applications," *International Journal of Electromagnetic Applications*, vol. 6, no. 2, pp. 49–55, 2016.

[6] M. Marzouk and Y. Rhazi, "Ultra-wideband compact fractal antenna for WiMAX, WLAN, C and X band applications," *Sensors*, vol. 23, no. 9, Art. no. 4254, 2023. https://doi.org/10.3390/s23094254

[7] V. Setia and K. K. Sharma, "Performance evaluation of triple-band microstrip antenna using hybrid-SRRs on truncated ground plane," *Defence Science Journal*, vol. 72, no. 4, pp. 379–386, Jul. 2022.

[8] X. L. Zheng, Q. F. Shi, D. F. Lu, and C. Y. Ji, "A novel tri-band ultra-wideband antenna with deformed split ring resonator for WLAN/WiMAX applications," *Applied Mechanics and Materials*, vols. 713–715, pp. 1265–1269, 2015. https://doi.org/10.4028/www.scientific.net/AMM.713-715.1265

[9] D. M. Elsheikh and E. A. Abdallah, "Compact multiband printed-IFA on electromagnetic band-gap structures for wireless applications," *International Journal of Microwave and Wireless Technologies*, vol. 5, no. 4, pp. 397–404, 2013. https://doi.org/10.1017/S1759078713000263

[10] E. Aparna, G. Ram, and A. Kumar, "5G mm-wave technology: Innovative design of integrating mm-wave wideband antenna with a compact CP microwave antenna for diverse applications," IEEE Access, vol. 12, pp. 54231–54241, 2024. https://doi.org/10.1109/ACCESS.2024.3389501

[11] S. Shankar and D. K. Upadhyay, "A fractal monopole antenna with dual-polarization reconfigurable characteristics for X-band applications," IEEE Access, vol. 11, pp. 117654–117664, 2023. https://doi.org/10.1109/ACCESS.2023.3311133

[12] J. Wang, Y. Li, and J. Wang, "A low-profile dual-mode slot-patch antenna for 5G millimeter-wave applications," IEEE Antennas and Wireless Propagation Letters, vol. 21, no. 3, pp. 517–521, Mar. 2022. https://doi.org/10.1109/LAWP.2022.3140747

[13] H. Yuan, F.-C. Chen, and Q.-X. Chu, "A wideband and high-gain dual-polarized filtering antenna based on multiple patches," IEEE Transactions on Antennas and Propagation, vol. 70, no. 10, pp. 9062–9071, Oct. 2022. https://doi.org/10.1109/TAP.2022.3177494

[14] M.-P. Shen, X. Geng, X. Yang, W.-W. Yang, and J.-X. Chen, "An extremely low-profile and longilineal dual-band shorted patch antenna for 5G mobile terminal applications," IEEE Antennas and Wireless Propagation Letters, vol. 23, no. 12, pp. 3621–3625, Dec. 2024. https://doi.org/10.1109/LAWP.2024.3454310

[15] Y. K. Choukiker, S. K. Sharma, and S. K. Behera, "Hybrid fractal shape planar monopole antenna covering multiband wireless communications with MIMO implementation for handheld mobile devices," *IEEE Transactions on Antennas and Propagation*, vol. 62, no. 3, pp. 1483–1488, Mar. 2014.

[16] Y. G. Adhiyoga, S. F. Rahman, C. Apriono, and E. T. Rahardjo, "Miniaturized 5G antenna with enhanced gain by using stacked structure of split-ring resonator array and magneto-dielectric composite material," *IEEE Access*, vol. 10, pp. 36121–36131, 2022. https://doi.org/10.1109/ACCESS.2022.3163285

[17] A. Azari, A. Skriverik, R. A. Sadeghzadeh, and H. Aliakbarian, "A super wideband dual-polarized Vivaldi antenna for 5G mmWave applications," IEEE Access, vol. 11, pp. 86512–86522, 2023. https://doi.org/10.1109/ACCESS.2023.3300040

[18] M. Li, Z. Sun, M.-C. Tang, and L. Zhu, "Broadband circularly polarized microstrip antenna with customized tilted beam based on index-modulated folded split ring resonator," IEEE Transactions on Antennas and Propagation, Early Access, 2024. https://doi.org/10.1109/TAP.2024.3353346

[19] Y. G. Adhiyoga, S. F. Rahman, C. Apriono, and E. T. Rahardjo, "Miniaturized 5G antenna with enhanced gain by using stacked structure of split-ring resonator array and magneto-dielectric composite material," IEEE Access, vol. 10, pp. 36121–36131, 2022. https://doi.org/10.1109/ACCESS.2022.3163285

[20] N. C. Pradhan, K. S. Subramanian, R. K. Barik, and S. Koziel, “Shielded HMSIW-based self-triplexing antenna with high isolation for WiFi/WLAN/ISM band,” IEEE Transactions on Circuits and Systems II: Express Briefs, vol. 70, no. 6, pp. 2273–2277, Jun. 2023. https://doi.org/10.1109/TCSII.2022.3231829

[21] T. Yang, J. Ren, B. Zhang, Y.-T. Liu, T. Ma, and Y. Yin, “Wideband diversity cylindrical dielectric resonator antenna based on multimode resonance,” IEEE Antennas and Wireless Propagation Letters, vol. 22, no. 9, pp. 1948–1952, Sep. 2023. https://doi.org/10.1109/LAWP.2023.3281478

[22] H. Wang and P. Wu, “Wideband MIMO antennas for 5G mobile terminals,” IEEE Open Journal of Antennas and Propagation, vol. 4, pp. 32–41, 2023. https://doi.org/10.1109/OJAP.2023.3234133